ADAPTIVE SNAKES FOR URBAN ROAD EXTRACTION

Junhee Youn[*]   James S. Bethel

Geomatics Area, School of Civil Engineering, Purdue University, West Lafayette, IN 47907-2051, USA
(**younj,bethel)@ecn.purdue.edu**

Commission III, WG III/4

Abstract:

For quickly populating GIS database, it is important to derive accurate and truly road information from imagery. In this paper, we describe the problem of urban road extraction from digital imagery using adaptive active contour models (Snakes). Our road extraction processing has three steps. First, we segment the image based on the dominant road directions. Second, we detect the road lines with the so called 'acupuncture method '. Finally, we refine the road edges by applying adaptive snakes to the corner desired approximation to extract the city block. During the process, we assume that the road network and block pattern in the city have a semi-regular grid pattern. For detecting the road lines, we exploit the distribution of edges in an urban area. Linear associated with roads are detected and these become the basis for initial approximations to road grid pattern for snakes based refinement. In order to accommodate variable line characteristics, we have developed an adaptive algorithm which locally modifies the weight of the energy terms. These ideas are applied to same actual urban imagery and the results are displayed and evaluated.

1. Introduction

Rapid and accurate generation of road data from imagery is an important issue in modern digital photogrammetry. Besides normal methods, there are two categories for road extraction. One is semi-automatic extraction and the other is fully automatic extraction.

In semi-automatic extraction, approximations are given manually and an automatic algorithm extracts the road. In Vosselman and de Knecht (1995), the operator provides the initial information (starting point and direction) and the subsequent road segments' positions are determined after profile matching in aerial imagery. Manually given data can be used as initial information for snake approaches; Gruen and Li (1997) proposed the method that the human operator select a few seed points and the linear feature is automatically extracted based on dynamic programming and least squares B-spline snakes. For the fully automatic approach, initial information can be given by other sources. Agouris *et al*.(2001) extended the traditional snakes to function in a differential mode and propose a framework to differentiate change detection from the older record of GIS. There are several approaches to use multi resolution aerial imagery for automatic methodologies. That approach usually extracts the lines in a reduced resolution image, and edges are extracted with the original high-resolution image. Both outputs are merged by using a rule based system (Heipke *et al.* 1995). And Baumgartner *et al*.(1999) composed road segment by using both resolution level with explicit knowledge about the road and grouped these segments iteratively, considering the local context.

So far, not so many research groups concentrate on road extraction in urban areas. For rural case, the geometry, radiometry and topology characteristics of roads are simple to describe, compared to urban areas. The most difficulties for urban road extraction are coming from the fact that material and shape (linear pattern) for non-road structures are very similar to the road. However, the road network in an urban area is usually semi-grid pattern. Price (1999) assumed that road network model is a regular grid form and the road has visible edges. He used two manually given intersecting road segments, which gave nominal information for the size and orientation of the grid. These segments are expanded with feature-based hypothesis and verification, and local context and a digital elevation model is used for refinement and verification of road segment. The grid characteristic for urban road networks is important assumption for our approach. Hinz *et al.* (2003) proposed a context-based decision making model for urban road detection, using complex relationships among roads buildings and vehicles. Here, context information about the urban road is mainly obtained from high-resolution imagery and a digital surface model.

In this paper, we present automatic road extraction in urban areas with adaptive snakes, for which initial seed points are calculated from a new approach for detecting road ways and intersections. Assuming urban networks to be a semi-grid pattern, there will be evident roads has several dominant directions. Dominant directions for roads can be determined based on the fact that road edges and building edges are usually parallel in the urban area. With dominant road directions, preliminary road lines are extracted for the snake refinement. These road lines are used an initial approximations. An adoptive strategy is derived wherein weighting factor vary with context of the road grid. Results are presented for some actual urban imagery.

2. Region-Based Image Segmentation

The Basic concept of this approach is to split the image into regions based on dominant road directions. In urban areas, most of the roads are straight and the road network often has a grid form, so the roads will exhibit dominant directions. Meanwhile, having the same grid pattern for the whole area is an ideal case. Certain parts of the area may have north-south direction roads and another part may be northeast-southwest direction roads. Considering such various grid patterns, a partitioning scheme is proposed. In our approach, the parent image is subdivided into four child image blocks (regions) when the parent image which covers an area with more than two dominant road directions.

The process has three steps; line segment extraction, dominant direction detection and image splitting with quadtree data structure.

2.1 Line Segment Extraction

Calculating a road's dominant road direction starts from extracting the line segments from the edge image since most of the roads in the urban area are line-shaped and edge detection is the most common method for extracting meaningful discontinuities imagery. We can't say extracted line segments from edges are all belonging to roads, because so many features in urban areas have also line shape edges. In addition, building edges and road edges are often parallel. So we can use most of the line shaped edges for calculating road directions even though they correspond for non-road features.

To extract the line segments, the Canny operator is applied to track all edges. Since the file size of modern imagery are quite large, we downsampled the imagery to work at reduced resolution. By reducing the resolution, much information is lost but to determine only the region's dominant direction, using a reduced resolution image is sufficient. The image for our study area and its detected edges are shown in Figure 1. The binary image for the canny detected edges is shown in Figure 1b, with black pixels represents the edges. Those edge pixels are for buildings, roads, trees, cars, and other features.

(a)   (b)
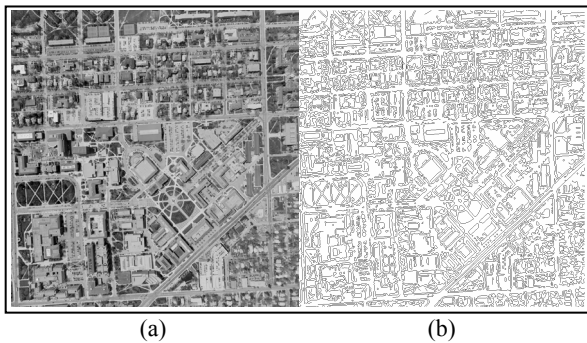
Figure 1: Image for study area and its edges. (a) Aerial image over Purdue Campus (b) Detected edges with reduced resolution image by canny algorithm
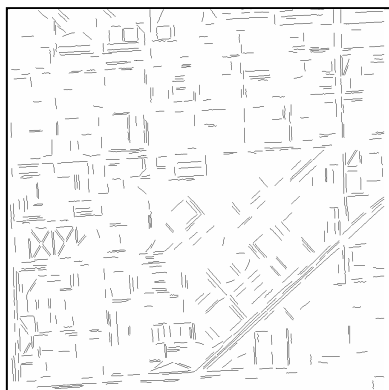
Figure 2. Extracted line segments with proposed algorithm

To get line-shaped edges (line segments), we propose following method. We use polar coordinate, which use ρ-θ, to parameterize the line.

First, we examine the search window, of size 20×20 pixel. This search window will adjoin ones by 3 pixels. Next, all components are 8-connected labeled to determine pixel groups

and each group's pixel elements ρ-θ. Based on calculated ρ-θ, pixels in the group are checked whether all pixels are on the line equation or not. If all pixels are on the line equation, this group is treated as "straight line". If not, the group will be eliminated.

Conditions for being treated as straight line are as follows;
- Length of group is more than limit
- At least one pixel of group touches the boundary of search window
- ρ-θ are calculated by using any two pixels in the group and all pixels should lie on this line (Tolerance is 1 pixel).
Extracted line segments are shown in Figure 2.

2.2 Dominant Direction Detection

We will subdivide an image block (parent region) into four quadrant image blocks (child regions) if the parent region has more than two dominant road directions. To decide about splitting or not, we must calculate the number of dominant directions in the region of interest. For determining the dominant direction in the scene, several approaches have been studied. Getting dominant directions in a scene is usually begun by straight line detection for most of the research groups. Then each line's gradient is calculated and line length is accumulated into a histogram. The problem is selecting dominant directions in this histogram.

Sohn and Dowman (2001) used a hierarchical histogram-clustering method to obtain dominant direction. They derived line angle information and quantized it into a histogram. Corresponding line length of each angle is accumulated to make many pixels contribute more to determine dominant angle peaks. Once the highest peak angle is obtained, angle discrepancies less than angle thresholds from peak angle are checked as one set. Their geometries are modified to conform to the peak angle. In subsequent searching, these modified and the checked sets are ignored. In this paper, we propose a modified hierarchical histogram-clustering method. We calculate the angle for each line, eliminate some lines with 90-degree filtering, threshold to make angle-pixel on histogram and then apply hierarchical histogram-clustering.

To calculate each line's angle, the Hough transform is used and Figure 3a is the result of calculating all line's angle and length. In Figure 3a and Figure 3b, circles represent each line's angle from 0 to 90 degree on the X axis, and length is represented by the Y axis.

(a)   (b)   (c)
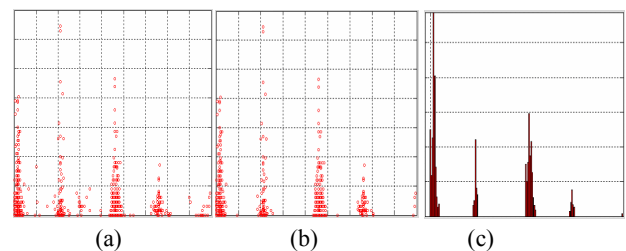
Figure 3. Angle – length relationship for line segments. (a) Angle and length for all line segments. (b) Result after 90-dgree filtering. (c) Histogram after 90-dgree filtering and threshold.

Our region of interest is an urban area and we already assume that urban roads form a kind of grid pattern. The grid is composed of two main directions which are perpendicular to each other. Also, because we searched a wide area, even if a certain line segment has a perpendicular segment, the two segments may have no relationship with the grid. Searching all line directions, we eliminated the lines that have no

perpendicular pair in region of interest. That is so called "90-degree filtering". Figure 3b is the result for 90-degree filtering. After 90-dgree filtering, we make a length threshold. If the length of a perpendicular pair is less than 1 percent of region's total length of line segments, that pair is eliminated. Figure 3c represents the filtered histogram in which the bin counts are the total number of pixels (length summation of line segments) and it is used for determine dominant direction of region. By this algorithm, we can expect non-road and non-building roof edges to be ignored.

From the Figure 3c, this region has four dominant directions about 0°, 45°, 90°, 135°, by intuitive inspection. We need mathematically separate it to determine the number of dominant direction. We used a hierarchical histogram-clustering method to determine the dominant angle set. After making dominant angle sets, we can calculate a representative angle for each set by following equations.

$$\theta_{dom} = \frac{\sum \theta_i \times n_i}{\sum n_i}$$

Where n_i is the length of line. As a consequence, the study area has four dominant directions, and the angles are 2.9°, 42.2°, 92.5°, and 132.1°.

2.3 Image Splitting with Quadtree Data Structure

The objective of Image splitting in this paper is to partition an image into regions until all regions have their own single pair of dominant directions. To partition the image, we applied the quadtree data structure. The following basic formulation is very similar to Gonzalez' (1992) Region-Oriented Segmentation method.

Let R represent the whole image region and it is divided into n sub regions liker R_1, R_2, ... R_n such that

(a) $\sum_{i=1}^{n} R_i = R$,

(b) R_i is a rectangular region, $i = 1, 2, \ldots n$,

(c) $R_i \cap R_j$ is null set for all i and j, $i \neq j$,

(d) $P(R_i) = TRUE$ if this region has only one pair of dominant direction.

Region is subdivided into four disjointed quadrants region if $P(R_i) = FALSE$. That means the R_i region has more than one pair of dominant direction. This splitting technique has a convenient representation form called the quadtree. Quadtree concept is represented in Figure 4.
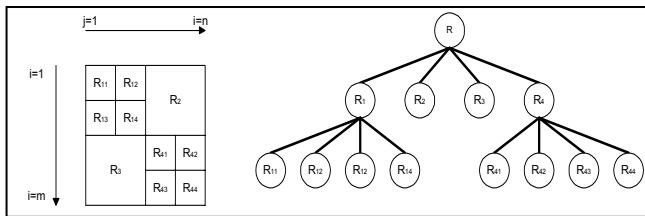
Figure 4. Concept for Quadtree image splitting

Let the size of the entire image be $m \times n$. First, calculate the entire image (R)'s dominant directions and if the entire region has only one pair of dominant directions, then image splitting is stopped. Otherwise, this region is subdivided into disjoint four quadrant regions (R_1, R_2, R_3, R_4). Second, if each R_i has only one pair of dominant directions, then splitting is stopped. Otherwise, each region is subdivided again into four quadrant disjoint rectangular regions of which size is $m/2 \times n/2$. This

process proceeds until all regions have their own pair of dominant directions or the region reaches a lower threshold limit. The region threshold can be predefined as a city block size (Min_{block}). The region segmentation result is shown in Figure 5. The red rectangle is the region which has one pair of dominant directions and the yellow region denote that dominant directions are not determined and splitting is stopped because the minimum size threshold has been reached. The reason why those regions don't have one pair of dominant directions is usually due to lack of line segments. In such cases of too few line segments, we skip 90 degree filtering and proceed to histogram clustering.
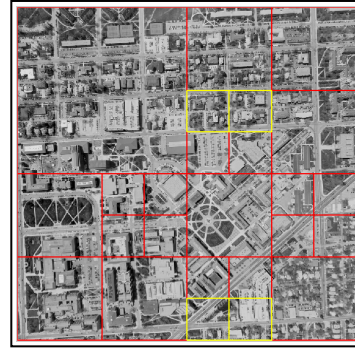
Figure 5. Image segmentation based on road directions

3. The position of the line on the road

Each region from the quadtree has its own two dominant road directions and, as mentioned above, those directions are parallel with road and building edges. Let's imagine two virtual needles that penetrate the two dimension edge image spaces and a compare a measure for both needles. We define a free passage to quantify this concept. Specifically, a needle which meets many edges will have a small free passage measure, whereas a needle which meets few or no edges will have a large free passage measure. Figure 6 illustrate the "needle piercing" process through an edge image. Because of the analogy with needle, we call this process the "Acupuncture Method".

Figure 6. Penetrating needles on the edge image

Replacing the needles as line equations on the edge image aligned with the dominant directions, and stepping exhaustively across the edge image, we can compute a free passage measure for each candidate line. We denote the two dominant directions θ_{d1} and θ_{d2}. The free passage measure for a fixed dominant direction and a given ρ is generated by following steps. Before implementing the steps, the range of ρ is defined as

$$\rho_{min} = Min\ (1,\ NL \cdot \cos\theta)$$
$$\rho_{max} = Max\ (NS \cdot \sin\theta,\ NL \cdot \cos\theta + NS \cdot \sin\theta\ )$$
$$\rho_{min} \leq \rho \leq \rho_{max}$$

where (NL, NS) is the size of image (number of lines, number of samples). Also, we define the function $N(X)$ which represents total number of elements for set X.

i) With ρ_i, calculate the line coordinates set P_i with point coordinates (l_j , s_j),

$$P_i = \begin{cases} 1 \le l_j \le NL \\ s_j = \dfrac{\rho_i - l_j \cdot \cos\theta}{\sin\theta} \end{cases} (45° < \theta < 135°)$$

$$P_i = \begin{cases} 1 \le s_j \le NS \\ l_j = \dfrac{\rho_i - s_j \cdot \sin\theta}{\cos\theta} \end{cases} (0° \le \theta \le 45° \; or \; 135° \le \theta < 180°)$$

ii) Next, we count the pixels where the edges coincide with the lines just described. For each line, i, overlay with each edge, k. The total number of coincident pixels (C_i) will be an indicator of "obstacles" encountered by that line. A large number of such obstacles will indicate that it is less likely to be a road feature, whereas a small number of obstacles will mean that it is more likely to be a road feature. The number of line/edge coincident pixels is

$$C_i = \bigcup_k (P_i \cap E_k)$$

where E_k is an edge pixel.

iii) We characterize the degree, to which the line is free from obstructing edges as,

$$F_i = \frac{N(P_i) - N(C_i)}{N(P_i)} \times 100 \quad (0 \le F_i \le 100).$$

A high value (near 100) of F_i is an indicator of a road. Repeating this process for each line we can make a graph of the free passage measure vs. line number. Peaks in this graph will very likely correspond to roads.

(a)	(b)	(c)
(d)	(e)	(f)
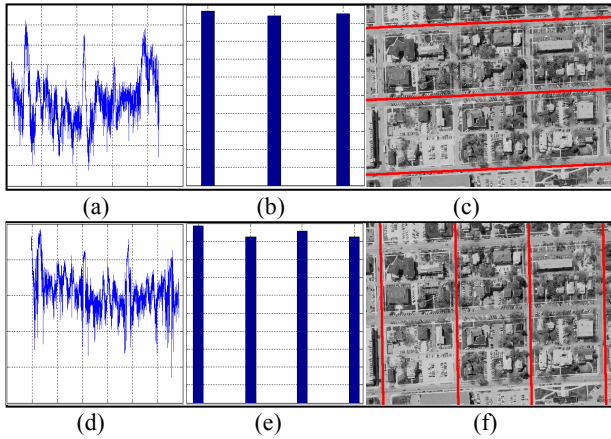
Figure 7. Result of acupuncture method on small example region. (a)~(c) are for θ_{d1}, and (a)~(c) are for θ_{d2}. (a) and (d) Free passage measure. (b) and (e) Clustering result. (c) and (f) Detected lines on the road.

Figure 7 is the example of applying acupuncture algorithm to one of the regions. In this region, the predetermined dominant road directions are 2.5° (θ_{d1}) and 91° (θ_{d2}). Figure 7a, 7b and 7c are for 2.5° case and others are for 91° case. Figure 7a and 7d show the graph that represents the relationship between line number and the free passage measure. In Figure 7a, Figure 7b,

Figure 7d and Figure 7e, the X axis represents the line number and the Y axis is the free passage measure.

From the graphs in Figure 7a and 7d, we select the peaks using modified hierarchical histogram clustering method. This method requires the user to specify a minimal block width. Figure 7b and 7e are the results for that method and determine the lines selected as roads. The θ_{d1} graphs yields 3 lines chosen as roads. The θ_{d1} graphs yields 4 lines. Applying the complete Acupuncture method to the study area yields the results shown in Figure 8. Those lines, interpreted as an urban road grid, will be used as initial approximations for the snake refinement.

Figure 8. Detected lines on the road by acupuncture method

4. Adaptive Snakes

Many research groups have tried to use snakes as a tool for rural area road extraction, and they have applied global energy coefficients. Applying global energy coefficients should be on the assumption that the linear features have similar curvature characteristics through the curve. Since the road structure for rural roads is not so complex, global energy coefficients perform well. Here, we propose adaptive snakes for which energy coefficients vary locally to accommodate urban area road extraction. First, we introduce the general solution for snakes and second, present the advantage of local varying energy coefficients. Third, we apply the proposed snakes to the study area with initial approximations which are generated in previous section. In this paper, we define 'global energy coefficients' as applying the same coefficients to the all nodes in one curve while 'local energy coefficients' means that coefficients vary locally.

4.1 General Solution for Snakes

The original concept for snakes (Active contour models) was introduced by Kass *et. al*(1988), and they define it as "A snake is an energy-minimizing spline guided by external constraint forces and influenced by image forces". Also, it can be defined as a movable curve in image domain controlled by internal forces (elastic and bending force etc.) and image forces which attract or repel the curve.

The Snakes can be modeled as a curve with time-dependent sequential list of nodes in two dimensions and define parametrically like

$$v(s,t) = (x(s,t), y(s,t)) \quad 0 \le s \le 1 \qquad (1)$$

,where t is current time or evolution step, s is proportional to the curve length, and x and y represent coordinates for nodes in the image domain. In this paper, the internal and external energy at any node are determined throughout the curve, and we find the optimum position of nodes with energy minimizing techniques. The energy of the snake can be written as a summation of internal and image energy as,

$$E_{snake} = E_{int}(v) + E_{img}(v) \qquad (2)$$

The internal energy controls the shape of the curve with geometric constraints and can be decomposed into a first and second order term as,

$$E_{int}(v) = \int_0^1 \alpha(s)|v_s(s,t)|^2 + \beta(s)|v_{ss}(s,t)|^2\, ds \cdot \qquad (3)$$

Here, coefficient α controls the elastic force of the curve and coefficient β controls the bending force of the curve. More detailed description for the internal energy will be stated next section. The image energy attracts the curve to the salient features in the image and is represented as,

$$E_{img}(v) = -\int_0^1 P(v(s,t))ds \qquad (4)$$

where $P(v(s, t))$ is function value corresponding to the feature of interest. In this paper, we focus on the edges as the salient feature, so $P(v(s, t))$ is the image gradient.

The total energy of the snake is written as

$$E_{snake} = \int_0^1 \alpha|v_s(s,t)|^2 + \beta|v_{ss}(s,t)|^2 - P(v(s,t))\, ds \cdot \qquad (5)$$

To minimize the energy functional, we use the *Euler-Lagrange* differential equations of the functional yielding the following simplified Euler evolution equation,

$$\gamma\frac{\partial v(s,t)}{\partial t} + \alpha v_{ss}(s,t) + \beta v_{ssss}(s,t) = -\frac{\partial P(v(s,t))}{\partial v} \qquad (6)$$

where γ represents the viscosity of the curve. The higher viscosity makes the evolution of the curve slower. v_{ss} is the second derivatives with respect to s. The temporal derivative can be numerically written as

$$\frac{\partial v(s,t)}{\partial t} = v(s,t) - v(s,t-1) \cdot \qquad (7)$$

Assuming external forces are changed very slowly with time step, substitute equation (7) to equation (6), equation (6) is rewritten as,

$$\alpha v_{ss}(s,t) + \beta v_{ssss}(s,t) + \frac{\partial P(v(s,t-1))}{\partial v} = -\gamma(v(s,t) - v(s,t-1)) \qquad (8)$$

Let V_t be a set of each nodes as,

$$V_t = \{v(i,t), i = 1,2...n\} \qquad (9)$$

where n is the total number of nodes in the curve.

Then, with equation (9) equation (8) can be rewritten in matrix form as

$$(A + \gamma I)V_t = \gamma V_{t-1} - \frac{\partial P(V_{t-1})}{\partial v} \qquad (10)$$

where the matrix A is a pentadiagonal banded matrix composed of α and β, and I is an n×n identity matrix. With the initial curve modeled by sequential list of nodes, the next curve is calculated by equation (10) iteratively and iteration will be stopped when total energy change is less than a threshold. Finally, we can find an optimal position of curve with this energy minimization technique.

4.2 Local Energy Coefficients for Urban city block detection

As stated in the previous section, snakes have internal energy components which are controlled by coefficients α and β. For accurate delineation of city blocks, boundaries of detected edges should remain in linear form in the preserve of concavities (parking lot near the side of city block) and convexities (parked car at the side of a city block). With the above mentioned characteristics, we know that the corner region is well suited for lower β compared with the sides of the block. Figure 9 shows us the difference between applying global energy coefficients (constants) versus local energy coefficients (context dependent). In Figure 9, the target for snakes simulates the example of a city block. The red line is a curve which is composed of blue nodes. Figure 9b is a result of applying global energy coefficients (constants) with initial contour in Figure 9a. Here, the corner area is well delineated, however snakes is sensitive to the concave and convex part. But applying different weighting coefficients to the corner and side area, an improved result is obtaining particularly in the side area.

(a)   (b)   (c)
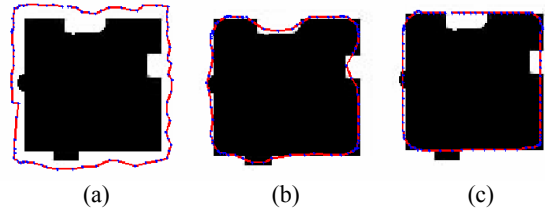
Figure 9. Global and local energy coefficients for snakes. (a) Initial contour (b) Global coefficient with $\alpha = 1$, $\beta = 0$. (c) Local coefficient: $\alpha = 1$, $\beta = 0$ for corner area and $\alpha = 300$, $\beta = 0$ for side area.

To use local weighting coefficients, we must have a priori knowledge about the point context before minimization. For our city block case, the point context (corner vs. side) is determined from the initialization. Davis *et al* (1995) tried to apply local coefficients for the snakes, and they had a little success because their resultant snake model did not fit with user expectation. Main problem for their approach is due to the unreliability of expectations for target shape. However, we can overcome that problem by using the 'detected lines on the road' obtained in the previous section. Detailed usage is described in the next section.

4.3 Applying Adaptive Snakes to City Block Delineation

Generally, initial curves for snakes are given by manually. However, road intersection, which are determined by detected lines on the road, generate the initial curves in our approach and also, they give us the information for the corner area. Seeing the result of detected lines in Figure 8, we focus on two facts; the

line intersections mostly correspond for road intersection, and these also coincide with block corners.

Energy minimization starts from making initial curve and proceeding with the refinement. Among all road intersection points, each four points become seed points for one initial curve. Based on these seed points, we insert nodes for which spacing is proportional to the distance from one seed point to another. Figure 10a is a detailed example of one initial curve with different point classification. A yellow dot is an intersection point, all blue points are inserted nodes, the large blue points are classified as corner area, and all points comprise the initial V_t in equation (9). We apply different internal weighting coefficients based on point location. We apply α and β value for corner area as 1 and 3, meanwhile give α 300 and β 0 for side area. With matrix A and the initial V_t, we iteratively solve for V_t for each time evolution step until the change of total energy is less than threshold. A result, which represents the city blocks, is in Figure 10b. To enhance the sensitivity to image forces, we use a spatial diffusion technique to spread the influence of the edges. Figure 11 is the result of applying adaptive snakes to the study area. We eliminate the non-converged curve during minimization.

(a) (b)
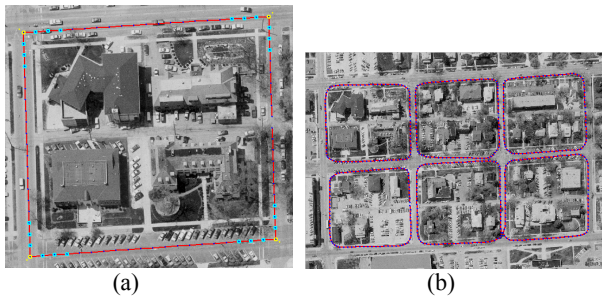
Figure 10. Adaptive snakes for urban road grids. (a) Local coefficients. (b) Detected city blocks.
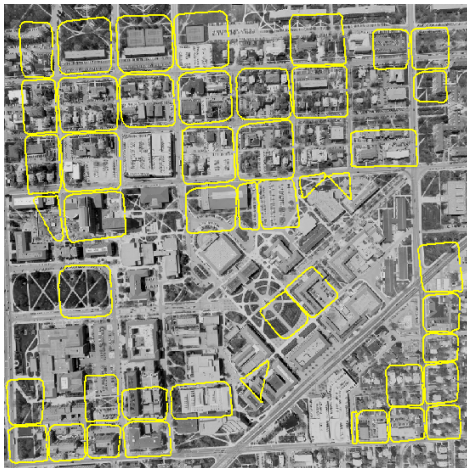
Figure 11. Detected city blocks in the study area

5. Conclusions

In this paper, we propose a new approach for urban road extraction. A basic assumption is that urban road network has a nominal grid pattern and a priori knowledge required is the approximate minimum size of the city block and approximate road width.

In region segmentation, we subdivide the region until all regions have only two dominant directions. By doing so, we can obtain each region's dominant road directions even if the road network has multiple grid patterns. The determined road directions were used for road detection. Searching the region with its road directions, we find the candidacy of lines on the road by using the 'acupuncture method'. These detected lines were used to construct initial approximations for the subsequent snake refinement. Line intersection were considered as road intersections and used for seed points for the snakes. Applying local weighting coefficients to the traditional snakes, we have developed an adaptive procedure well fitted for urban city block delineation. Our future work will focus on achieving better stability in the numerical estimation, improving the adaptive algorithm, and comparing different methods of computing the steps in the line fitting.

References

Agouris, P., A. Stefanidis, and S. Gyftakis, 2001. Differential snakes for change detection in road segments, *Photogrammetric Engineering & Remote Sensing*, 67(12):1391-1399.

Baumgartner, A., C. Steger, H. Mayer, W. Eckstein, and H. Ebner, 1999. Automatic road extraction based on multi-scale, grouping, and context, *Photogrammetric Engineering and Remote Sensing*, 65(7):777-785.

Davis, D.N., K. Natarajan, and E. Claridge, 1995. Multiple energy function active contours applied to CT and MRI images of the brain, *Proceedings of the 5th IEE Conference on Image Processing and its Applications*, Edinburgh, UK, pp. 114-118.

Gonzalez, R., and R. Woods, 1992. *Digital Image Processing*. Addison Wesley Publishing Company, Reading, Massachusetts, 458 p.

Gruen, A., and H. Li, 1997. Semi-automatic Linear feature extraction by dynamic programming and LSB-snakes. *Photogrammtric Engineering & Remote Sensing*. 63(8): 985–995.

Heipke, C., C. Steger, and R. Multhammer, 1995. A Hierarrchical Approach to Automatic Road Extraction From Aerial Images, *SPIE – Aerosense 1995 Symposium*, 17-21 April, Orlando, USA, Vol. 2486, pp.222-231.

Hinz, S., A. Baumgartner, H. Mayer, C. Widemann, and H. Ebner, 2003. Road Extraction Focusing on Urban Area, *Automatic Extraction of Man-Made Objects from Aerial and Space Images(III)*, (E. Baltsavias, A. Grün, and L. Van Gool, editors), A.A. Balkema Publishers, Lisse, The Netherlands, pp. 255-265.

Kass, M., A. Witkin, and D. Terzopoulos, 1988. Snakes: Active contour models, *International Journal of Computer Vision*, 1(4):321-331.

Price, K., 1999. Road Grid Extraction and Verification, *International Archives of Photogrammetry and Remote Sensing*, 32(Part 3/2w5):101-106.

Sohn, G., and I.J Dowman, 2001. Extraction of buildings from high-resolution satellite data, *Automatic Extraction of Man-Made Objects From Aerial and Space Images(III)* (E. Baltsavias, A. Grün, and L. Van Gool, editors), A.A. Balkema Publishers, Lisse, The Netherlands, pp. 345-355.

Vosselman, G., and J. de Knecht, 1995. Road tracing by profile matching and Kalman filtering, *Automatic Extraction of Man-Made Objects from Aerial and Space Images* (A. Gruen, O. Kuebler, and P. Agouris, editors), Birkhaeuser Verlag, Berin, Germany, pp. 265 – 274.